16-kDa Prolactin Inhibits Endothelial Cell Migration by Down-Regulating the Ras-Tiam1-Rac1-Pak1 Signaling Pathway

Sok-Hyong Lee,[1] Jeannette Kunz,[5] Sue-Hwa Lin,[6] and Li-yuan Yu-Lee[1,2,3,4]

Departments of [1]Immunology and [2]Medicine, Section of Immunology Allergy and Rheumatology, [3]Department of Molecular and Cellular Biology, Biology, [4]Program in Cell and Molecular Biology, and [5]Department of Molecular Physiology, Baylor College of Medicine; and [6]Department of Molecular Pathology, M. D. Anderson Cancer Center, Houston, Texas

Abstract

Angiogenesis plays a key role in promoting tumorigenesis and metastasis. The 16-kDa fragment of prolactin (16k PRL) is an NH_2-terminal natural breakdown fragment of the intact 23-kDa prolactin and has been shown to have potent antiangiogenic and antitumor activities. The mechanism(s) involved in the action of 16k PRL in endothelial cells remains unclear. In this study, we showed that 16k PRL reduced rat aortic endothelial cell (RAEC) migration in a wound-healing assay and in a Matrigel tube formation assay, suggesting that 16k PRL inhibits endothelial cell migration, an important activity involved in angiogenesis and tumorigenesis. We further investigated how 16k PRL attenuates endothelial cell migration. We first showed that RAEC migration is mediated through the Rho GTPase Rac1, as Rac1 inhibition by the Rac1-specific inhibitor NSC27366 or Rac1 knockdown by small interfering RNA both blocked RAEC migration. We next showed that 16k PRL reduced the activation of Rac1 in a concentration-dependent manner. Furthermore, 16k PRL inhibition of Rac1 is mediated through the suppression of T lymphoma invasion and metastasis 1 (Tiam1) and its upstream activator Ras in a phosphoinositide-3-kinase–independent manner. 16k PRL also down-regulated the phosphorylation of the downstream effector of Rac1, p21-activating kinase 1 (Pak1), and inhibited its translocation to the leading edge of migrating cells. Thus, 16k PRL inhibits cell migration by blocking the Ras-Tiam1-Rac1-Pak1 signaling pathway in endothelial cells. [Cancer Res 2007;67(22):11045–53]

Introduction

The 23-kDa prolactin (23k PRL) is a peptide hormone synthesized and secreted primarily by the pituitary gland, but is also produced in many extrapituitary tissues (1). 23k PRL can be further proteolyzed into fragments of various sizes. The 16-kDa fragment of prolactin (16k PRL) is a predominant NH_2-terminal prolactin fragment, and is present in the hypothalamus, pituitary gland, mammary gland, and kidney in humans (2–4). 16k PRL can be generated by the cleavage of 23k PRL by matrix metalloproteases from human chondrocytes (5) and cathepsin D in various tissues and cell types (3, 6).

In contrast to 23k PRL, which has angiogenic effects in pathogenic conditions such as rheumatoid arthritis (7) or breast cancer (8), 16k PRL has potent antiangiogenic effects. 16k PRL was shown to inhibit the basal, basic fibroblast growth factor (bFGF)–, and vascular endothelial growth factor (VEGF)–stimulated proliferation of endothelial cells (9, 10). 16k PRL inhibited the growth of new capillaries in a chick embryo chorioallantoic membrane assay (9, 11) and blocked rat retinal neovascularization (12). Furthermore, 16k PRL was shown to have antitumor activities *in vivo*. Bentzien et al. (11) showed that 16k PRL inhibited the tumorigenicity of HCT116 cells in a Rag1(−/−) mouse model. Kim et al. (13) showed that 16k PRL reduced the tumorigenicity of DU145 and PC-3 human prostate cancer cells in a xenograft nude mouse model. As angiogenesis is required for tumor progression *in vivo*, 16k PRL likely inhibits tumor growth through its antiangiogenic activity.

Several studies have explored the mechanisms by which 16k PRL exerts its antiangiogenic effects on endothelial cells. 16k PRL stimulates plasminogen activator inhibitor-1 (PAI-1), a potent antiangiogenic factor in bovine brain endothelial cells (BBEC; ref. 10). 16k PRL induces caspase-dependent apoptosis with the activation of nuclear factor κB in BBECs (14). Our studies suggest that 16k PRL may inhibit tumor angiogenesis by attenuating the production of nitric oxide (NO), an endothelial cell survival factor, in rat aortic endothelial cells (RAEC; ref. 15). In RAEC, 16k PRL reduces interleukin (IL)-1β–inducible *iNOS* gene transcription through inhibition of the p38 mitogen-activated protein kinase (MAPK)–Stat1-IRF-1 pathway (15).

Endothelial cell proliferation and migration are critical properties that drive vessel formation, homeostasis, and angiogenesis (16). Members of the Rho family GTPases, Cdc42, Rac1, and RhoA, are essential factors for cell polarity, motility, adhesion, and actin-mediated changes in cell shape (17). Among the Rho GTPases, Rac1 is critical for cell motility and actin-remodeling (17, 18). Transfection with small interfering RNA (siRNA) oligonucleotides against Rac1 inhibited cell migration in response to a wound scratch in glioblastoma cells (19), whereas overexpression of constitutively active Rac1 (V12) facilitated fibroblast migration and promoted leading edge actin-rich ruffling (20). Other studies have implicated the Ras-Raf pathway in 16k PRL inhibition of VEGF-induced proliferation in endothelial cells (21), but little is known about whether this pathway is involved in 16k PRL regulation of endothelial cell migration. In this report, we show that 16k PRL inhibits endothelial cell migration in both a wound healing and a Matrigel tube formation assay. Furthermore, by using a series of biochemical assays and immunofluorescence image analyses, we show that 16k PRL inhibits the Ras-Tiam1-Rac1-Pak1 signaling pathway in attenuating endothelial cell migration.

Materials and Methods

Reagents, antibodies, and recombinant 16k PRL. Recombinant human 16k PRL was purified as previously described (22). IL-1β (R&D

Note: Supplementary data for this article are available at Cancer Research Online (http://cancerres.aacrjournals.org/).

Requests for reprints: Li-yuan Yu-Lee, Department of Medicine, One Baylor Plaza, Houston, TX 77030. Phone: 713-798-4770; Fax: 713-798-5780; E-mail: yulee@bcm.tmc.edu.

doi:10.1158/0008-5472.CAN-07-0986

Systems), Rac1 inhibitor (NSC27633), and phosphoinositide-3-kinase (PI3K) inhibitor (wortmannin; Calbiochem), and antibodies for Rac1 (Upstate), β-actin, T lymphoma invasion and metastasis 1 (Tiam1), phosphorylated p21-activating kinase 1 (Pak1, Thr^{423}; Santa Cruz Biotechnology), Ras, phospho-Akt, and Akt (Cell Signaling) were purchased from commercial sources.

Cell culture. RAECs (23) were maintained in DMEM with 10% fetal bovine serum (FBS; Invitrogen) and 50 μg/mL of gentamicin (Sigma-Aldrich; ref. 15). Human umbilical vein endothelial cells were maintained in M-199 medium containing 10% FBS, 10% bovine calf serum (Invitrogen), 50 μg/mL of gentamicin, and 20 μg/mL of endothelial cell growth supplement (BD Biosciences).

Endothelial cell migration assay. RAEC (2.5×10^5 cells) were grown to confluence in a 12-well plate, placed in medium containing 1% serum for 24 h, and scratched using either a 200 μL or 1 mL pipette tip. Serum was increased to 5% to facilitate cell migration. RAEC migration was recorded using a Nikon TE2000E microscope system (Nikon Instrument). The area of wound sealing was calculated using NIH ImageJ software.

Matrigel tube formation assay. Matrigel (BD Biosciences; 100 μL) was added to a 96-well plate and incubated for 12 h at 37°C for solidification. RAEC (2.5×10^4 cells) were added to the Matrigel in DMEM containing 5% FBS. Tube formation was recorded using the Nikon microscope system.

Rac1 siRNA transfection. RAEC (2.5×10^5 cells) were mixed with 200 nmol/L of siRNA for Luciferase or rat Rac1 (siGENOME SMARTpool M-080171-01-0010, NM_134366; Dharmacon) in 100 μL of Amaxa nucleofector solution V (Amaxa), and transfected in an Amaxa nucleofector (model AAD-1001). Rac1 protein depletion was determined by Western blot analysis.

Preparation of pull-down substrates. The Rac1-binding substrates were generated as described (24). The Rac1-binding domain in Pak1 (PBD; amino acids 67–150) was amplified by PCR using sense primer (*Bam*HI site underlined): 5′ CGC GGATCC AAGAAAGAGAAAGAGCGGCCAGAG 3′ and antisense primer (*Eco*RI site underlined): 5′ CCG GAATTC CTA ATGACT-TATCTGTAAAGC 3′, subcloned into p-GEX2T (Amersham) to generate the GST-Pak1-PBD vector, and confirmed by sequencing. GST-Rac1G15A vector was a gift from Dr. Krister Wennerberg (Cytoskeleton, Denver, CO) and GST-Tiam1 Ras-binding domain (RBD; amino acids 721–840) vector was a gift from Dr. Junji Yamauchi (National Research Institute for Child Health and Development, Setagawa, Japan; refs. 25, 26).

GST pull-down assay. RAEC were subjected to multiple wound scratches using a 200 μL pipette tip and treated simultaneously with 2.5 ng/mL of IL-1β (WS/IL-1β) for a more robust activation of Rac1 (27). Cells were harvested in 1.5 mL of lysis buffer [25 mmol/L HEPES (pH 7.5), 150 mmol/L NaCl, 1% NP40, 10 mmol/L $MgCl_2$, 1 mmol/L EDTA and 10% glycerol, 10 μg/mL leupeptin, 10 μg/mL aprotinin, 1 mmol/L sodium fluoride, and 1 mmol/L sodium orthovanadate]. Cell lysates (500 μg) were incubated with 15 μg of GST-Pak1 PBD beads for 1 h at 4°C with rocking. Bound proteins were resolved on a NuPage 4% to 12% Bis-Tris gradient gel (Invitrogen) and transferred to nitrocellulose membranes (Bio-Rad). Active GTP-bound Rac1 was determined by Western blot analysis. Similarly, active Tiam1 was determined using GST-Rac1G15A beads and active Ras was determined with GST-Tiam1 RBD beads in GST pull-down assays (25, 26).

Western blot analysis. RAEC subjected to WS/IL-1β were harvested in 1.5 mL of lysis buffer [20 mmol/L Tris (pH 7.4), 100 mmol/L NaCl, 5 mmol/L EDTA, and 0.5% Triton X-100] supplemented with 1 mmol/L of phenylmethylsulfonyl fluoride and a protease-inhibitor cocktail (Sigma). Cell lysates (10–20 μg) were blotted with antibodies for Rac1 (1:1,000), β-tubulin (1:3,000), phospho-Pak1 (Thr^{423}; 1:500), Pak1 (1:1,000), Tiam1 (1:800), Ras (1:1,000), phospho-Akt (Ser^{473}; 1:1,000), or Akt (1:1,000). For secondary antibodies, goat anti-mouse or rabbit horseradish peroxidase antibody (1:2,000; Santa Cruz Biotechnology) was used. Immunoblots were developed by enhanced chemiluminescence (Pierce), and quantified using a Storm960 PhosphorImager (Molecular Dynamics).

Immunoprecipitation. RAEC were prepared as described for Western blotting, except that the buffer also contained 1 mmol/L of serine/threonine phosphatase inhibitor and 1 mmol/L of tyrosine inhibitor (Sigma). Cell lysates (750 μg) were incubated with 2 μg of anti-Pak1 antibody overnight at 4°C. Protein G agarose beads (20 μg) were added for 3 h at 4°C. Immunoprecipitated proteins were analyzed by Western blotting using anti–phospho-Pak1(Thr^{423}) antibody followed by reblotting using anti-Pak1 antibody.

Immunofluorescence imaging. RAEC cells were cultured on glass coverslips coated with poly-D-lysine (1 mg/mL, 70,000–15,000 Da; Sigma) and subjected to WS/IL-1β. Cells were fixed in PEM buffer [80 mmol/L PIPES (pH 7.0), 1 mmol/L EGTA, 1 mmol/L $MgCl_2$], and permeabilized with ice-cold ethanol for 5 min at −20°C. The coverslips were blocked in 2% bovine serum albumin and 2% goat serum in TBS-T [20 mmol/L Tris (pH 7.4), 150 mmol/L NaCl, 0.05% Tween 20] for 1 h at room temperature, and incubated with anti–phospho-Pak1(Thr^{423}) antibody (1:200) overnight at 4°C, followed by goat anti-rabbit IgG–conjugated Alexa-Fluor 488 (1:500; Molecular Probes) for 2 h at room temperature. The coverslips were then incubated with 10 nmol/L of rhodamine-conjugated phalloidin for 30 min and counterstained using SlowFade Light Antifade Kit with 4′,6-diamidino-2-phenylindole (Molecular Probes). Images were obtained with the Nikon microscope system and compiled using Adobe Photoshop 9.0 (Adobe Systems).

Statistical analysis. All results were confirmed in multiple independent experiments, with each time point or condition assayed in duplicates or triplicates within each experiment. Densitometry data were analyzed by using Student's *t* test and expressed as mean ± SE. $P < 0.05$ was considered statistically significant.

Results

16k PRL attenuates endothelial cell migration in response to wound scratch. To examine the effect of 16k PRL on endothelial cell migration, we employed a well-established wound-healing assay to characterize the cell migration response in RAEC. A confluent layer of RAEC was first incubated overnight in medium containing 1% serum, a wound scratch was introduced, medium containing 5% serum was added to stimulate migration, and the percentage of wound sealing was observed over an 8-h time course. Control RAEC initiated migration into the wound area after 2 h, reaching 50% and 70% sealing at 6 and 8 h, respectively, after wound scratch (Fig. 1*A, a* and *f*). To evaluate whether 16k PRL affects endothelial cell migration, RAEC cells were treated with 20 nmol/L of 16k PRL at the same time with the wound scratch. 16k PRL–treated RAEC only showed ~20% sealing 8 h after wound scratch (Fig. 1*A, b* and *f*), suggesting that 16k PRL attenuated wound-induced cell migration. 16k PRL also attenuated the migration of primary human umbilical vein endothelial cells in the wound-healing assay (see Supplementary Fig. S1).

16k PRL inhibits IL-1β–inducible endothelial cell migration in response to wound scratch. We previously showed that 16k PRL inhibits IL-1β–inducible signaling in RAEC (15), but the effect of 16k PRL on IL-1β−inducible endothelial cell migration has not been examined. Treatment of RAEC with IL–1β following wound scratch significantly increased the rate of wound sealing compared with that of control cells at each of the time points examined (Fig. 1*A, c* and *f*). IL-1β–treated RAEC reached 50% wound sealing after ~4 h compared with 6 h for control cells (Fig. 1*A, f*). The addition of 16k PRL to IL-1β significantly blocked RAEC migration (Fig. 1*A, d* and *f*). These observations indicate that IL-1β enhances RAEC migration in response to wound scratch, and that 16k PRL inhibits IL-1β–inducible RAEC migration.

Rac1 mediates endothelial cell migration in response to wound scratch. Cell migration is largely regulated by Rac1 activity (17). To analyze whether Rac1 may be involved in the migration of RAEC in the wound healing assay, RAEC were treated with the Rac1-specific inhibitor NSC23766, which blocks Rac1 binding to its guanine nucleotide exchange factor Tiam1 in fibroblasts (28).

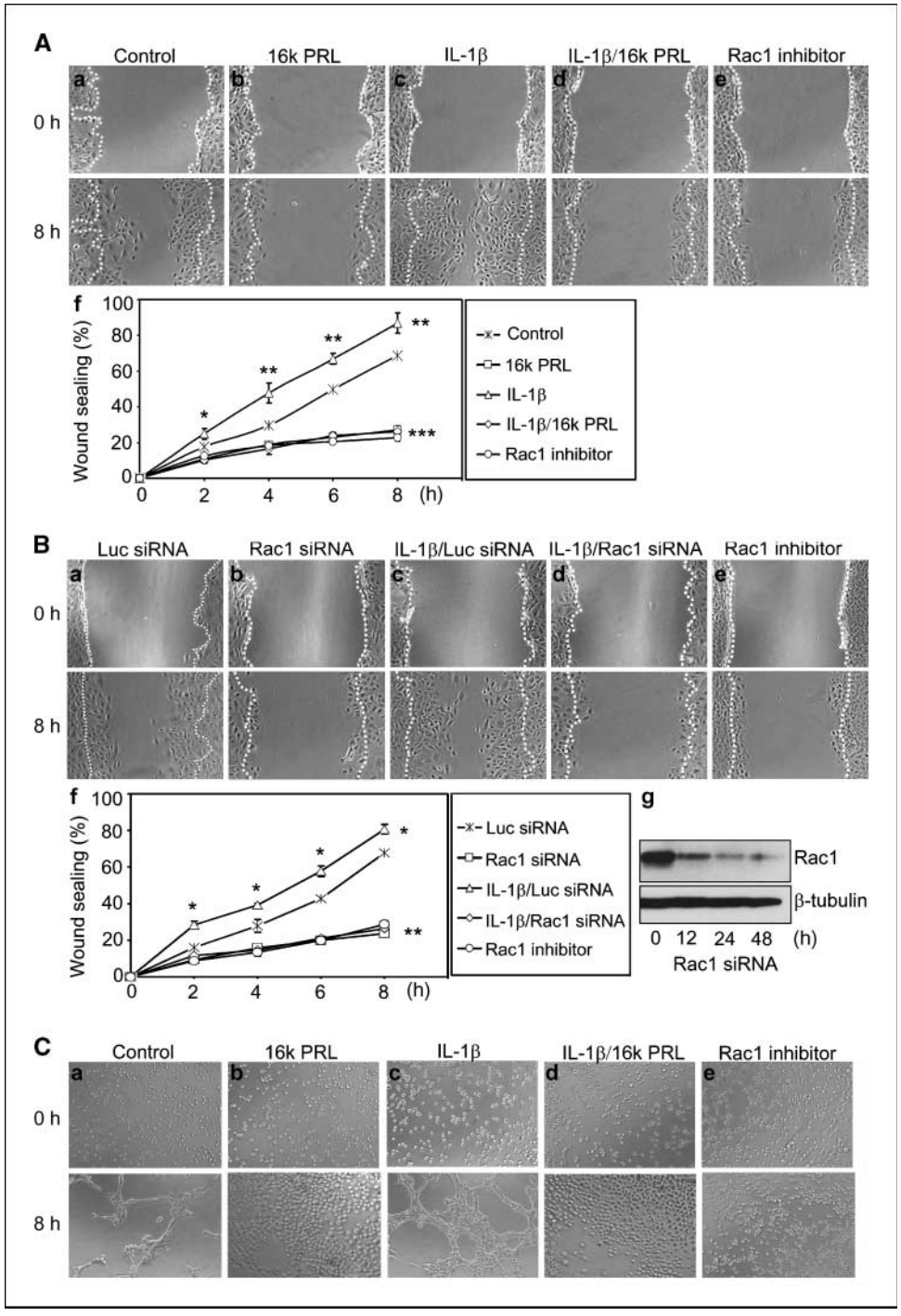

Figure 1. 16k PRL reduces aortic endothelial cell migration. *A,* RAEC wound healing assay. RAEC were grown to 80% to 90% confluence in a 12-well plate, and incubated in medium containing 1% FBS overnight. RAEC monolayers were scratched (*dotted lines*) with a 1 mL pipette tip and cultured with medium containing 5% FBS to facilitate cell migration. Cells were treated with 5% FBS medium alone (*Control*; *a*), 20 nmol/L of 16k PRL (*b*), 2.5 ng/mL of IL-1β (*c*), IL-1β plus 16k PRL (*d*), or 50 μmol/L of NSC27366, a Rac1 inhibitor (*e*). Cell migration was recorded by phase contrast microscopy over an 8-h time course after wound scratch. Representative images of wound sealing at 0 and 8 h after wound scratch. The level of cell migration into the wound scratch was quantified as the percentage of wound sealing and compared against that of control cells at each time point (*f*). *, $P < 0.05$; **, $P < 0.01$; ***, $P < 0.001$. Values represent averages ± SE of three independent measurements along the wound scratch. Note the percentages of wound sealing under the different conditions at 8 h after the wound scratch were reproducibly observed in at least four independent experiments. *B,* Rac1 siRNA. RAEC (2.5×10^5 cells) were transfected for 48 h with 200 nmol/L of control Luciferase siRNA (*a*) or 200 nmol/L of rat Rac1 siRNA (*b*). Wound healing assays were done as described in *A*. Luc siRNA control (*a*), Rac1 siRNA (*b*), 2.5 ng/mL of IL-1β plus Luc siRNA (*c*), IL-1β plus Rac1 siRNA (*d*), and 50 μmol/L of NSC27366 Rac1 inhibitor (*e*). The percentage (*f*) of wound sealing was quantified as in *A*. *, $P < 0.01$; **, $P < 0.001$. Rac1 depletion by Rac1 siRNA (*g*). RAEC cell lysates (15 μg) from a Rac1 siRNA time course were analyzed by Western blotting with anti-Rac1 antibody. β-Tubulin was used as a loading control. *C,* RAEC Matrigel tube formation assay. RAEC (2.5×10^4 cells/well) were seeded on solidified Matrigel, and treated with medium containing 5% FBS (control; *a*), 20 nmol/L of 16k PRL (*b*), 2.5 ng/mL of IL-1β (c), IL-1β plus 16k PRL (*d*), or 50 μmol/L of NSC27366 Rac1 inhibitor (*e*). Tube formation was recorded by phase contrast microscopy at 0 and 8 h after seeding. Representative data from one of three independent experiments.

Treatment of RAEC with 50 μmol/L of NSC23766 inhibited wound scratch–induced cell migration (Fig. 1*A, e* and *f*), suggesting that Rac1 is involved in RAEC migration. To further strengthen this observation, we knocked down Rac1 levels by incubating cells for 48 h with Rac1 siRNA oligonucleotides (Fig. 1*B, g*), and analyzed wound-sealing over an 8-h time course after wound scratch. Control RAEC treated with Luciferase siRNA completed 70% sealing 8 h after wound scratch (Fig. 1*B, a* and *f*). In contrast, RAEC treated with Rac1 siRNA were significantly blocked in their ability to seal the wound area (Fig. 1*B, b* and *f*). The degree of inhibition of wound sealing mediated by Rac1 siRNA was comparable to that observed with the Rac1 inhibitor (Fig. 1*B*, compare *b* with *e*, and see *f*) in RAEC. These studies show that Rac1 levels as well as Rac1 activity are involved in RAEC migration in a wound-healing assay.

Rac1 mediates IL-1β–inducible endothelial cell migration in response to wound scratch. We next determined if the IL-1β–inducible RAEC migration might be mediated through Rac1. In control RAEC treated with Luciferase siRNA, IL-1β stimulation showed nearly 80% wound sealing 8 h after wound scratch (Fig. 1*B, c* and *f*). The IL-1β–inducible wound sealing activity was reduced, after Rac1 knockdown, to a similar level as that observed with the Rac1 inhibitor (Fig. 1*B*, compare *d* with *e*, and see *f*) in RAEC.

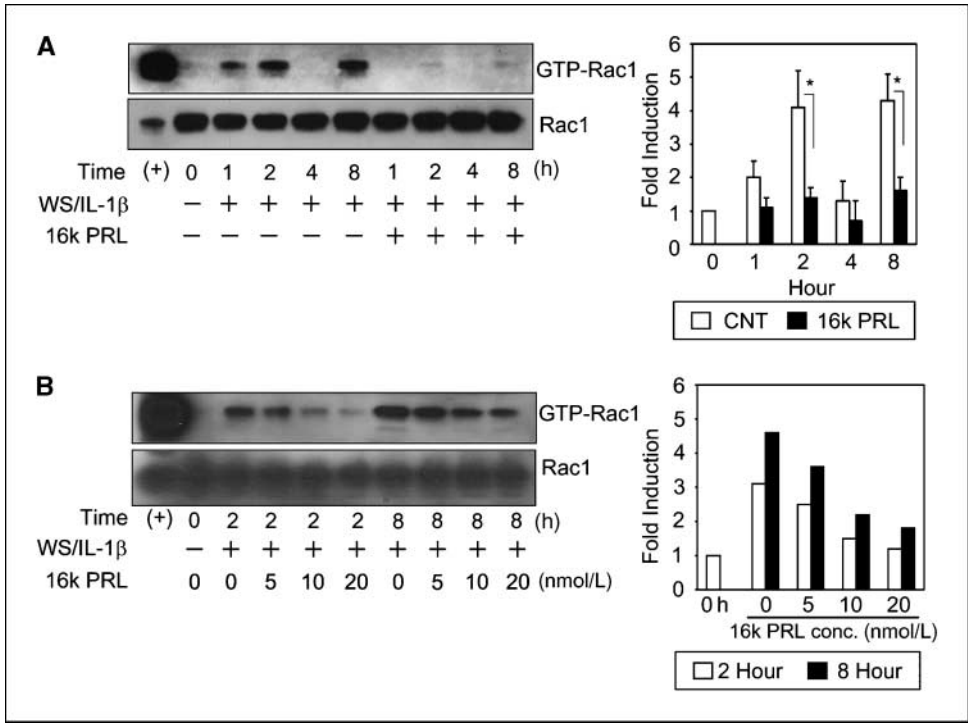

Figure 2. 16k PRL down-regulates Rac1 activation in response to wounding in aortic endothelial cells. RAEC were grown to 80% to 90% confluence in a 10-cm dish and cultured as described in Fig. 1. In this and subsequent experiments, cells were subjected to a combination treatment of multiple wound scratches generated with a 200 μL pipette tip and the addition of 2.5 ng/mL of IL-1β (*WS/IL-1β*). *A,* Rac1 pull-down assay. RAEC were treated with WS/IL-1β in the presence or absence of 20 nmol/L of PRL for the indicated times. Cell extracts (750 μg) were incubated with 10 μg of GST-Pak1-PBD and bound active GTP-Rac1 was analyzed by Western blotting using anti-Rac1 antibody. For a positive control, 100 μmol/L of nonhydrolyzable GTPγS was added to control RAEC extracts (+). For a negative control, 100 μmol/L of GDP was added to RAEC extracts (data not shown). Total Rac1 levels in cell lysates (15 μg) were unchanged in a parallel Western blot using anti-Rac1 antibody. The average fold induction ±SE in GTP-Rac1 levels was determined from four independent experiments. *, $P < 0.01$. *B,* 16k PRL inhibits Rac1 activation in a dose- and time-dependent manner. RAEC treated for 2 or 8 h by WS/IL-1β were incubated with increasing concentrations of 16k PRL as indicated. GTP-Rac1 levels were determined by GST pull-down assays as in *A* and fold induction was determined from two independent experiments.

These studies indicate that IL-1β–inducible wound sealing activity is mediated through Rac1, as Rac1 knockdown prevented IL-1β–mediated RAEC migration.

16k PRL inhibits tubular network formation in Matrigel. We further investigated the effects of 16k PRL on endothelial cell migration by using the Matrigel matrix tube formation assay, another well-established system for examining angiogenesis under *in vitro* conditions (29). Control RAEC cultured in Matrigel for 8 h fused into extensive tubular networks (Fig. 1*C, a*). In contrast, 16k PRL–treated RAEC were unable to form tubular networks (Fig. 1*C, b*). These observations show that 16k PRL inhibits RAEC migration in the Matrigel endothelial cell tube formation assay. The addition of IL-1β stimulated a more robust Matrigel tube formation response than that observed in control cells (Fig. 1*C, c*), further supporting the observation that IL-1β induces endothelial cell migration. The addition of 16k PRL to IL-1β blocked RAEC Matrigel tube formation (Fig. 1*C, d*). Treatment of RAEC with 50 μmol/L of NSC23766 inhibited Matrigel tube formation (Fig. 1*C, e*), suggesting that Rac1 is also involved in the RAEC tubular network formation in Matrigel.

16k PRL down-regulates Rac1 activation in response to wound scratch. The cell migration assays (Fig. 1) suggest that 16k PRL may target the Rac1 pathway in endothelial cells. To examine whether the effect of 16k PRL on RAEC migration is mediated through Rac1 at the biochemical level, we analyzed Rac1 activation by using a GST pull-down assay. In this assay, GTP-bound active Rac1 is selectively retained by binding to the Pak1-binding domain (PBD) of its substrate Pak1 in the GST-Pak1 PBD matrix. Treatment of RAEC with either wound scratch or IL-1β alone induced a weak activation of Rac1 (data not shown). To generate a more robust activation of Rac1, we devised a protocol (WS/IL-β) that combines multiple wound scratches with the addition of 2.5 ng/mL of IL-1β (27). In control RAEC, WS/IL-1β induced a rapid but transient activation of Rac1 at 1 to 2 h (Fig. 2*A*). Rac1 activation returned to basal levels at 4 h but increased again at 8 h (Fig. 2*A*), a time corresponding to active cell migration as observed in the wound healing assay (Fig. 1*A*). Thus, WS/IL-β induced a biphasic 4- to 5-fold activation of Rac1 in endothelial cells. In contrast, RAEC subjected to WS/IL-β in the presence of 16k PRL were unable to activate Rac1 at either the 2- or 8-h time point (Fig. 2*A*), suggesting that 16k PRL inhibited Rac1 activation in endothelial cells. Further analysis showed that 16k PRL inhibited Rac1 activation in both a time- and dose-dependent manner, with 20 nmol/L of 16k PRL exhibiting the most pronounced inhibition of Rac1 activation (Fig. 2*B*). Together, these findings suggest that 16k PRL inhibits WS/IL-β–induced Rac1 activation in endothelial cells.

16k PRL down-regulates Tiam1 activation in response to wound scratch. We further analyzed the upstream signaling molecules that regulate Rac1 activation as potential targets of 16k PRL inhibition. Based on well-described Rac1 activation pathways in neuronal and fibroblast cultures (26), the guanine nucleotide exchange factor Tiam1 is an upstream activator of Rac1. When active Tiam1 binds to Rac1, it facilitates the release of GDP from Rac1 and stabilizes the nucleotide-free state of Rac1. GTP binds to

Rac1 and activated GTP-Rac1 is then released from Tiam1 (25). Because Tiam1 has a higher affinity for nucleotide-free Rac1, we measured active Tiam1 by using a nucleotide-free mutant of Rac1 (Rac1G15A) as the binding matrix in a GST pull-down assay (25). RAEC treated with WS/IL-1β showed biphasic activation of Tiam1 at 2 and 8 h after wound scratch, reaching 4- to 5-fold Tiam1 activation at 8 h (Fig. 3*A*). The biphasic timing of Tiam1 activation mirrors the biphasic activation of Rac1 (Fig. 2*A*), which is consistent with Tiam1 being an upstream activator of Rac1. In contrast, RAEC treated with WS/IL-1β in the presence of 16k PRL were unable to activate Tiam1 (Fig. 3*A*). The kinetics of Tiam1 inhibition by 16k PRL (Fig. 3*A*) parallels that of Rac1 inhibition by 16k PRL (Fig. 2*A*), suggesting that 16k PRL reduces Tiam1-mediated Rac1 activation in endothelial cells.

16k PRL reduces Ras activation in response to wound scratch. Ras is a member of the Rho family of G proteins that plays an important role in regulating Tiam1 and Rac1 activities in Schwann cells during migration (26). In addition, Ras can form a complex with Tiam1 in HEK293 cells (26). To see whether Ras activates the Tiam1-Rac1 pathway in endothelial cells, we transfected constitutively active Ras (L61) into RAEC and found that Ras highly induced Rac1 activation in endothelial cells (data not shown). Next, to determine whether Ras is activated in response to WS/IL-1β, we measured Ras activation by using the RBD (amino acids 721–840) of Tiam1 in a GST pull-down assay (26). In control RAEC, Ras was activated in a biphasic manner, first at 1 to 2 h and then at 8 h in response to WS/IL-1β (Fig. 3*B*). The more rapid kinetics of Ras activation at 1 h after WS/IL-1β is consistent with Ras being the upstream activator of Tiam1 (Fig. 3*A*) and Rac1 (Fig. 2). In contrast, RAEC treated with WS/IL-1β in the presence of 16k PRL were unable to activate Ras (Fig. 3*B*). Thus, 16k PRL reduces WS/IL-1β–induced Ras activation in endothelial cells. Together, our studies suggest that 16k PRL attenuates WS/IL-1β–induced RAEC migration by inhibiting the Ras-Tiam1-Rac1 pathway in endothelial cells.

16k PRL reduces Pak1 phosphorylation and phospho-Pak1 translocation in response to wound scratch. A major downstream effector of Rac1 is Pak1. Pak1 becomes activated by autophosphorylation at Thr^{423} upon binding of GTP-Rac1 to the Pak-binding domain (30). Active Pak1 phosphorylates and inactivates the myosin light chain kinase, and phosphorylates and activates LIM kinase 1. Inactivation of the myosin light chain kinase blocks actin-myosin contraction (31), whereas activated LIM kinase 1 further phosphorylates cofilin and inactivates cofilin-mediated actin depolymerization (32). In this way, activated Pak1 allows actin-myosin elongation and actin polymerization, which together are crucial for lamellipodia formation and cell migration. We next examined whether 16k PRL inhibits RAEC migration through inhibition of the Rac1-Pak1 pathway. Treatment of RAEC with WS/IL-1β–induced Pak1 autophosphorylation on Thr^{423} from 2 to 8 h (Fig. 4*A*), in which the slight delay relative to Rac1 activation (Fig. 2*A*) is consistent with Pak1 being a downstream target of Rac1. The elevated level of phospho-Pak1 at 4 h may be due to signaling from other Rho GTPases that also activate Pak1 phosphorylation (33). 16k PRL significantly decreased Pak1 autophosphorylation across all time points (Fig. 4*A*). These results show that 16k PRL inhibits WS/IL-1β–induced Pak1 autophosphorylation in endothelial cells.

Pak1 phosphorylation is required for the formation of the actin bundles and meshwork in the lamellipodia and phospho-Pak1 is localized to the lamellipodia at the leading edge during cell migration (34). To visualize phospho-Pak1 translocation into the lamellipodia, RAEC were examined by immunofluorescence microscopy. We chose to examine cell morphology 8 h after wound scratch, a time corresponding to a 4- to 5-fold increase in phospho-Pak1 levels in RAEC (Fig. 4*A*). In control RAEC, phospho-Pak1 clearly translocated to the leading edge lamellipodia in response to wound scratch (Fig. 4*B, a, arrows*). The accumulation of phospho-Pak1 was coincident with that of actin at the lamellipodia (Fig. 4*B, a, Merge*). In contrast, RAEC treated with

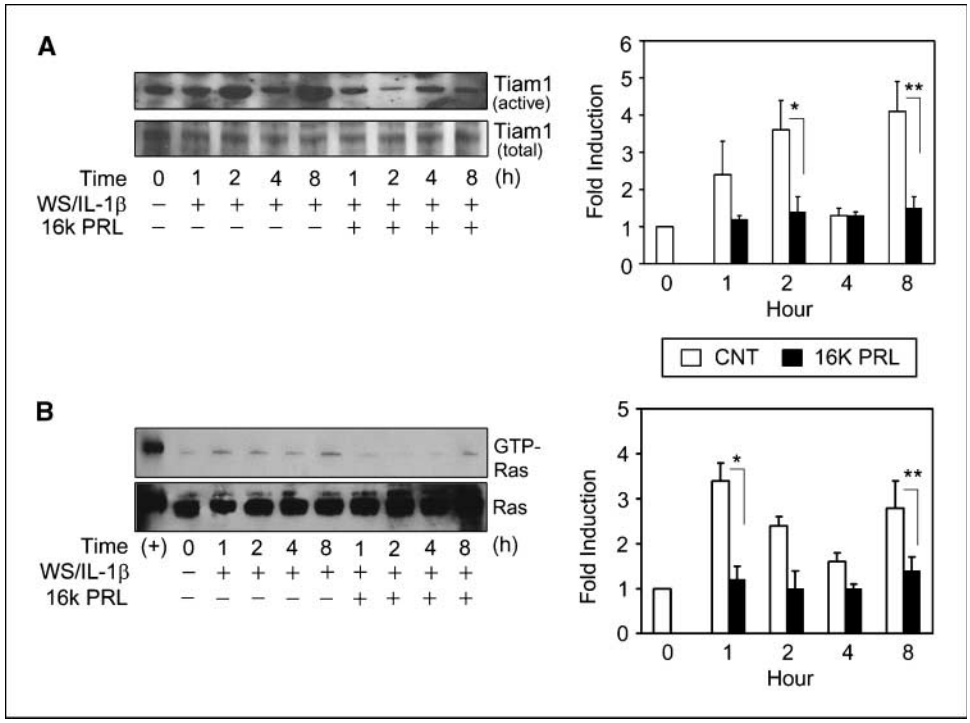

Figure 3. 16k PRL inhibits Tiam1 and Ras activation in response to wounding in aortic endothelial cells. *A,* Tiam1 pull-down assay. RAEC treated as in Fig. 2 were harvested at 0, 1, 2, 4, and 8 h in the presence or absence of 20 nmol/L of 16k PRL. Cell lysates (1.2 mg) were incubated with 15 μg of GST-Rac1G15A and active Tiam1 was analyzed by Western blotting using anti-Tiam1 antibody. For a positive control, 15 μg of NIH/3T3 cell extract was used (data not shown). Total Tiam1 levels in cell lysates (20 μg) were unchanged as shown in a parallel Western blot. The average fold induction ±SE in active Tiam1 was determined from three independent experiments. *, $P < 0.05$; **, $P < 0.01$. *B,* Ras pull-down assay. RAEC were treated as in *A* and cell lysates (750 μg) were incubated with 10 μg of GST-Tiam1-RBD beads. Active GTP-Ras was analyzed by Western blotting using anti-Ras antibody. For positive controls, 15 μg of Nb2 T cell lysates were used (+). Total Ras levels in cell lysates (15 μg) remained essentially unchanged in a parallel Western blot using anti-Ras antibody. The average fold induction ±SE of active GTP-Ras was determined from three independent experiments. *, $P < 0.01$; **, $P < 0.05$.

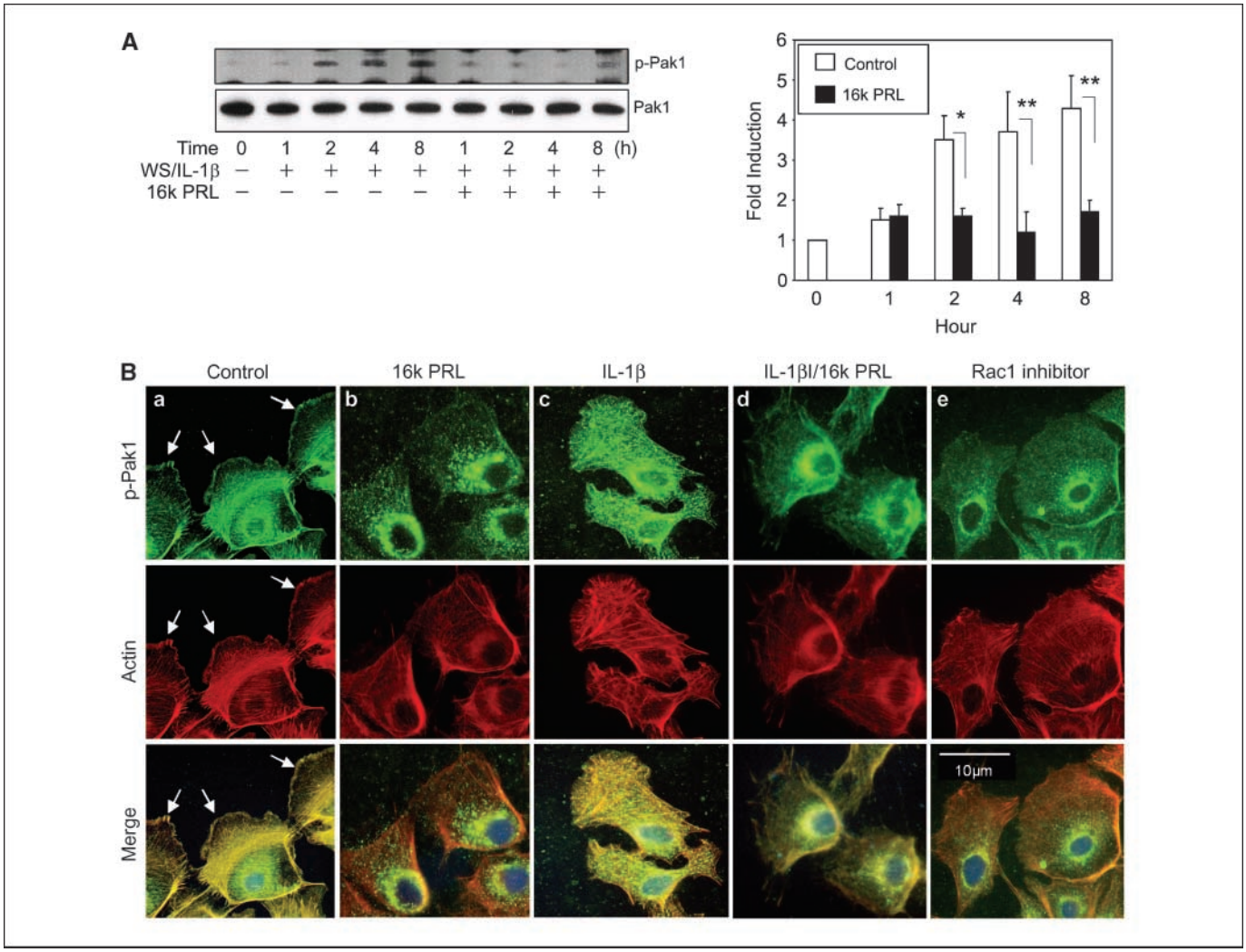

Figure 4. 16k PRL down-regulates Pak1 phosphorylation and phospho-Pak1 translocation in aortic endothelial cells. *A,* phospho-Pak1 immunoprecipitation. RAEC treated as in Fig. 2 were harvested at 0, 1, 2, 4, and 8 h in the presence or absence of 20 nmol/L of 16k PRL. Cell lysates (750 μg) were immunoprecipitated with 1.5 μg of anti-Pak1 antibody and Western blotted using anti–phospho-Pak1 antibody (*top*). Total Pak1 levels were unchanged as determined by reblotting with anti-Pak1 antibody. Sorbitol-treated COS cell extract was used as a positive control (data not shown). The average fold induction ±SE of phospho-Pak1 levels was determined from three independent experiments. *, $P < 0.05$; **, $P < 0.01$. *B,* immunofluorescence microscopy. RAEC in a 12-well plate was subjected to wound scratch with a 1 mL pipette tip and treated with either medium alone (*Control*; *a*), 16k PRL (*b*), IL-1β (*c*), IL-1β plus 16k PRL (*d*), or Rac1 inhibitor NSC23766 (*e*). Cells were fixed, permeabilized, and incubated with anti–phospho-Pak1 antibody (*green*), phalloidin for actin (*red*), and counterstained with 4′,6-diamidino-2-phenylindole for nuclei (*blue*). *Arrows,* lamellipodia at the leading edge of migrating cells. Images are representative of three independent experiments. Bar, 10 μm.

wound scratch plus either 16k PRL (Fig. 4*B, b*) or the Rac1 inhibitor (Fig. 4*B, e*) did not show phospho-Pak1 translocation to or actin accumulation at the leading edge lamellipodia.

RAEC subjected to WS/IL-β showed elevated accumulation of phospho-Pak1 in the lamellipodia as well as a robust formation of actin network (Fig. 4*B, c*). In contrast, 16k PRL blocked WS/IL-β–inducible translocation of phospho-Pak1 as well as actin network formation at the leading edge lamellipodia (Fig. 4*B, d*), which is consistent with the general lack of phospho-Pak1 present in these cells after 16k PRL treatment (Fig. 4*A*). Thus, 16k PRL reduces Pak1 phosphorylation and phospho-Pak1 translocation to the leading edge lamellipodia of migrating REAC in response to wounding.

16k PRL does not interfere with PI3K signaling in RAECs. Rac1 can be activated through both PI3K-dependent and -independent mechanisms (35, 36). To examine whether WS/IL-1β–induced Rac1 activation might also be mediated through PI3K, we preincubated RAEC for 1 h with 100 nmol/L of wortmannin, a PI3K-specific inhibitor, before WS/IL-1β treatment. A 2-h incubation with WS/IL-1β induced Rac1 activation (Fig. 5*A, lane 2*), and this activation was inhibited by the Rac1 inhibitor NSC23766 but not by wortmannin (Fig. 5*A, lane 4* versus *lane 3*). In contrast, phosphorylation of Akt, a well-described downstream target of PI3K, was inhibited by wortmannin but not by the Rac1 inhibitor (Fig. 5*A, lane 3* versus *lane 4*). These results showed that the PI3K-Akt pathway is not involved in the WS/IL-1β response in endothelial cells.

To directly show that 16k PRL does not affect PI3K activity, RAEC were subjected to WS/IL-1β in the presence of wortmannin and/or 16k PRL. The presence of 16k PRL, whether pretreated (pre) or cotreated (co) with WS/IL-1β (Fig. 5*B, lanes 3* to *5*), did not affect phospho-Akt expression in RAEC. Furthermore, 16k PRL also did not affect wortmannin inhibition of phospho-Akt expression (Fig. 5*B, lanes 6* and *7*). These results show that 16k PRL does not interfere with PI3K-Akt signaling in endothelial cells. Thus, RAEC

response to WS/IL-1β does not involve PI3K activity, and 16k PRL inhibition of Tiam1-Rac1 signaling does not involve PI3K activity in endothelial cells.

Discussion

Cell migration is a critical characteristic of angiogenesis, and reorganization of the cytoskeleton is an important aspect in cell migration. The small family of Rho GTPases plays an important role in cell migration by transducing signals that regulate changes in actin and microtubule cytoskeletal networks (17). We showed that 16k PRL attenuates wound scratch–induced endothelial cell migration by targeting the Rac1 signaling pathway. First, 16k PRL interfered with endothelial cell migration and tubular network formation in a Matrigel matrix. Second, 16k PRL inhibited WS/IL-1β–inducible endothelial cell migration and tubular network formation. Third, 16k PRL inhibited WS/IL-1β–induced Rac1 activation. The extent of 16k PRL-mediated interference was comparable to those observed by blocking Rac1 with either a Rac1-specific inhibitor NSC23766 or by knocking down Rac1 by siRNA. Fourth, 16k PRL inhibited Ras signaling to the guanine nucleotide exchanger Tiam1 that regulates Rac1 activation. Fifth, 16k PRL inhibited the phosphorylation of Pak1, a downstream effector of Rac1, as well as phospho-Pak1 translocation to the leading edge of migrating cells. Thus, 16k PRL attenuates endothelial cell migration through blocking the Ras-Tiam1-Rac1-Pak1 pathway (Fig. 6).

Rac1 plays a central role in mediating cell migration (18). In fibroblasts, constitutively active Rac1 augments whereas a dominant negative form of Rac1 or Rac1-specific inhibitor interferes with lamellipodia formation and cell motility (17). In endothelial cells, our wound scratch/IL-1β protocol generated biphasic activation of Rac1, with a first peak between 1 and 2 h and a second peak at 8 h (Fig. 2). The endothelial cell response to IL-1β stimulation is very rapid, as we have previously observed p38 MAPK activation within 5 min and Stat1 activation within 30 min of IL-1β stimulation of RAEC (15). In the absence of wounding, IL-1β alone can stimulate Rac1 but to a limited extent at 2 h (data not shown). The recovery of cell-to-cell contact after wound scratch and the formation of a new line of cells at the wound edge at around 2 h after wounding could also contribute to the first peak of Rac1 activation (data not shown). By 8 h after WS/IL-1β, RAEC migrated into the wound, and wound sealing was ~80% completed (Fig. 1). Palacios and D'Souza-Schory reported elevated Rac1 activation at 8 h with increased cell motility after epithelial cell scattering (37). Thus, IL-1β stimulation coupled with the initial cellular response to wounding might contribute to the first peak of Rac1 activation (Fig. 2), whereas the second peak of Rac1 activity might be correlated with increased cell motility (Fig. 1). Interestingly, 16k PRL efficiently blocked Rac1 activation at both the early and later time points, suggesting that 16k PRL could attenuate IL-1β signaling (15), cell-to-cell contact and cell motility in RAEC.

In line with the biphasic activation of Rac1, WS/IL-1β induced biphasic activation of upstream activators of Rac1, the guanine nucleotide exchange factor Tiam1 (Fig. 3*A*) and its upstream activator Ras (Fig. 3*B*) in RAEC. The kinetics of Ras activation slightly preceded that of Tiam1, which is consistent with Ras signaling through Tiam1 to Rac1 (38). The direct activation by Ras of Tiam1-Rac1 has been observed in neuronal Schwann cells (26). Depending on the cell type and stimulus (35, 36), Ras can activate Rac1 through PI3K signaling and PI3K could mediate Tiam1-Rac1 activation. We showed that in RAEC, WS/IL-1β does not activate the PI3K pathway and that 16k PRL inhibits Ras signaling in a

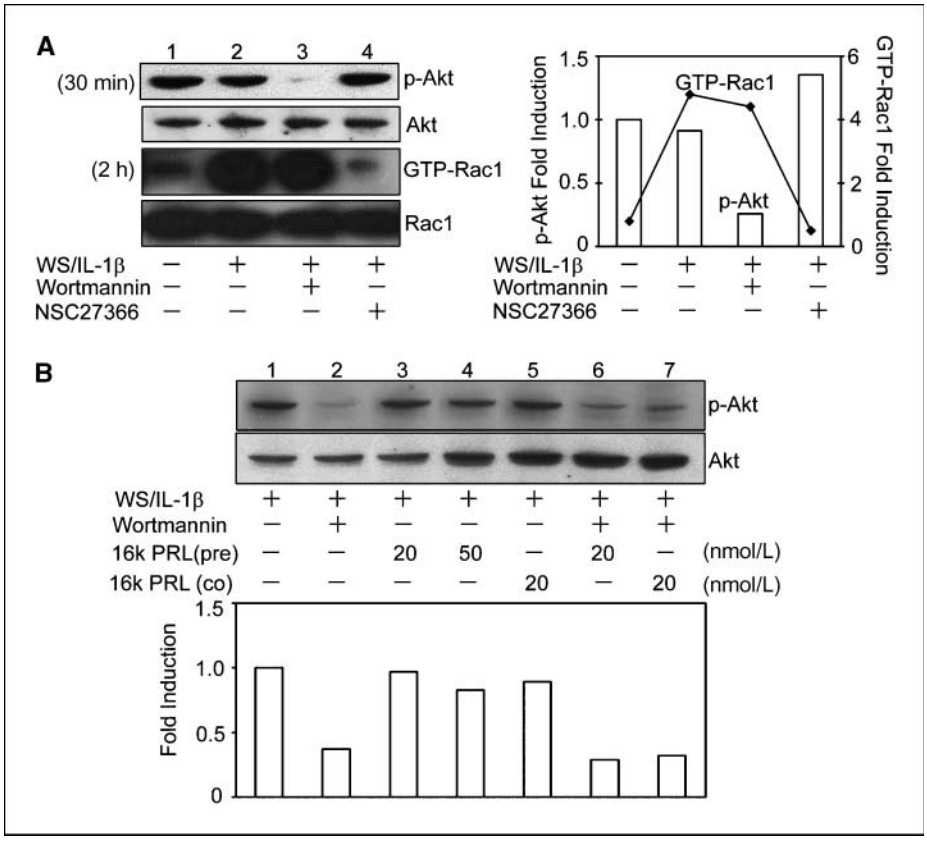

Figure 5. 16k PRL does not affect PI3K signaling in aortic endothelial cells. *A,* phospho-Akt and Rac1 analyses. RAEC were treated essentially as in Fig. 2, except that cells were preincubated with 100 nmol/L of wortmannin, a PI3K inhibitor, or 50 μmol/L of NSC23766 Rac1 inhibitor for 1 h before WS/IL-1β treatment. For phospho-Akt analyses, cells were harvested 30 min after treatment. Cell lysates (20 μg) were immunoblotted with anti–phospho-Akt antibody followed by reblotting with anti-Akt antibody. For Rac1 analysis, cells were harvested 2 h after treatment, and 500 μg lysates were analyzed by GST-Pak1 PBD pull-down assays for active GTP-Rac1. Total Rac1 levels were unchanged as determined by Western blotting. The average fold induction of phospho-Akt and Rac1 levels was determined from two independent experiments. *B,* PI3K signaling. RAEC were treated as in *A*, except that 20 or 50 nmol/L of PRL was added 1 h before (pre) or 20 nmol/L of PRL was added at the same time (co) as WS/IL-1β. Cell lysates were harvested 30 min after the addition of wortmannin and analyzed for phospho-Akt and total Akt levels as in *A*.

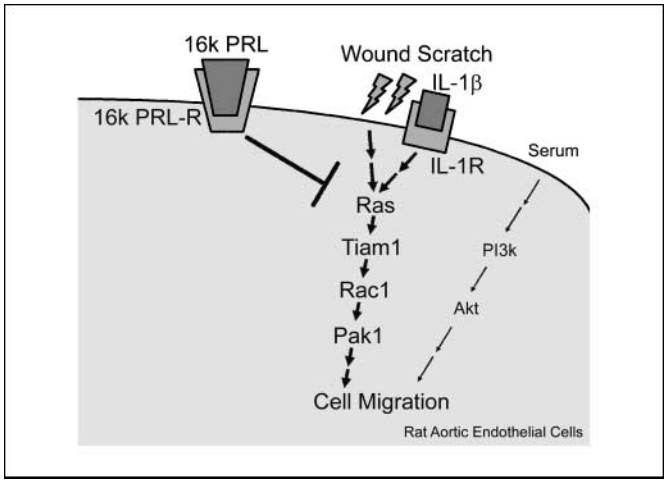

Figure 6. Model of 16k PRL regulation of cell migration in aortic endothelial cells. In our wound healing model, IL-1β binding to the IL-1β receptor (*IL-1R*) plus wound scratch (WS/IL-1β) together stimulates the biphasic activation of the Ras signaling pathway in RAEC. IL-1β most likely contributes to the early (~1 h) stimulation of Ras activity whereas wound-induced cell migration correlates with a second peak (~8 h) of Ras activation. The biphasic activation of Ras leads to the biphasic stimulation of Tiam1 and Rac1, which activates the downstream effector Pak1. 16k PRL binding to an as-yet unidentified 16k PRL receptor (*16k PRL-R*) inhibits WS/IL-1β–inducible Ras activation, resulting in the inhibition of the Tiam1-Rac1-Pak1 signaling pathway and reduction of phospho-Pak1 translocation to the lamellipodia at the leading edge of migrating cells. WS/IL-1β does not activate the PI3K-Akt pathway and 16k PRL does not interfere with PI3K-Akt signaling in endothelial cells. Thus, 16k PRL attenuates endothelial cell migration through the inhibition of the Ras-Tiam1-Rac1-Pak1 pathway.

PI3K-independent manner (Fig. 5). D'Angelo et al. reported that 16k PRL inhibits VEGF-induced Ras-Raf-1-MEK-ERK activation pathway in BBEC (21). Thus, 16k PRL targets Ras signaling in response to either a growth factor– (21) or wound-induced activation in endothelial cells (Fig. 6; ref. 15).

Actin and microtubule cytoskeletal networks play a central role in regulating membrane extensions in lamellipodia and cell polarity, respectively, and thereby regulate directed cell movement (17, 20). Rac1 regulates actin polymerization and lamellipodia protrusions at the leading edge whereas Cdc42 controls filopodia protrusions and cell polarity (20, 39). A major common downstream effector for Rac1 and Cdc42 is Pak1 (39, 40). Phospho-Pak1 stimulates the formation of actin meshwork in the leading edge lamellipodia (34), a process that is crucial for cell migration. In WS/IL-1β–treated RAEC, instead of the biphasic activation kinetics observed for Ras-Tiam1-Rac1 signaling, phospho-Pak1 levels were increased at 2 h and remained elevated till 8 h (Fig. 4*A*). The sustained Pak1 activation could be due to the combined activities of Rac1 and Cdc42. The robust formation of actin-rich filopodia and lamellipodia in WS/IL-1β–treated RAEC would support this idea (Fig. 4*B*). Whether 16k PRL blocks the activities of both Rac1 and Cdc42 in inhibiting phospho-Pak1 activation remains to be determined. 16k PRL blocked phospho-Pak1 activation, its translocation into the lamellipodia, and formation of the actin meshwork at the lamellipodia (Fig. 4*B*), suggesting that 16k PRL diminished the dynamic actin organization at the lamellipodia to attenuate cell migration. Additionally, 16k PRL–treated cells also exhibited a higher degree of misorientation of the microtubule-organizing center relative to the direction of cell migration (data not shown), which indicates that 16k PRL may also affect cell polarity through the effects of Cdc42 activity (39). Taken together, 16k PRL may reduce actin dynamics at the lamellipodia, cell polarity, as well as cell-to-cell contacts through down-regulation of Rho GTPase activities to attenuate endothelial cell migration.

16k PRL is a strong antiangiogenic and antitumor agent (9, 11, 13) that inhibits growth factor–mediated proliferation (9) and differentiation (15, 41, 42) of endothelial cells and induces apoptosis in endothelial cells (3, 14). Inhibition of tumor growth by 16k PRL in two *in vivo* cancer models (11, 13) was correlated with a reduction in microvessel density, which is consistent with 16k PRL inhibition of the endothelial compartment in tumors (4, 42). We and others found that 16k PRL inhibits capillary tube formation in Matrigel (Fig. 1*C*) as well as in type I collagen gels (9). Rac1 has been suggested to mediate endothelial cell tube formation by regulating the expression of cell adhesion molecules vascular cell adhesion molecule-1, intercellular adhesion molecule-1, and E-selectin (43, 44). Whether 16k PRL–mediated Rac1 down-regulation (Fig. 2) affects endothelial cell adhesion properties, which in turn regulate endothelial cell migration and vessel network formation (Fig. 1), remains to be determined.

Additional mechanisms for inhibition of angiogenesis by 16k PRL have been suggested. 16k PRL inhibits bFGF-mediated urokinase activity (urokinase type plasminogen activator; uPA) through the induction of PAI-1, the inhibitor of uPA, in BBEC (41). In breast cancer cells, the Rac1-MKK3-p38 MAPK pathway stimulates uPA expression via stabilization of uPA mRNA (45). It would be interesting to determine if 16k PRL inhibition of Rac1 contributes to the down-regulation of uPA expression in endothelial cells. 16k PRL has also been shown to inhibit the production of NO, a factor important for endothelial cell survival, migration, and capillary tube formation (46). 16k PRL antagonizes VEGF-inducible endothelial nitric oxide synthase activation (42) as well as IL-1β–inducible iNOS expression (15) to block NO production in endothelial cells. Preliminary studies showed that the NO inhibitor L-NAME prevented RAEC migration in both the wound healing and Matrigel tube formation assays to a similar extent as that observed with Rac1-specific inhibitor (data not shown). These studies raise the interesting possibility that the NO-mediated pathway (15) and the Rac1-mediated pathway (Fig. 6) may collaborate to promote endothelial cell migration and angiogenesis.

Recent studies have elucidated a role for 16k PRL as a natural inhibitor of ocular angiogenesis as one way to maintain avascularity in the eye (47). The loss of angiogenesis inhibitors may lead to retinal neovascularization observed in retinopathy of prematurity, diabetic retinopathy, and macular degeneration (48). Interestingly, many tissues can process 23k PRL into 16k PRL through the local release of cathepsin D (6). The pathologic outcome of excessive 16k PRL was manifested in postpartum cardiomyopathy in which cardiomyocyte cathepsin D processing of high levels of 23k PRL present after delivery led to decreased myocardial capillary density, degeneration of cardiac capillary network, and reduced cardiac function in postpartum women (49). Thus, 16k PRL is a potent endogenous "vasoinhibin" that regulates vascular functions (48).

16k PRL likely functions through a cell surface receptor that is distinct from the 23k PRL receptor (50). Although the receptor(s) for 16k PRL has not been identified, progress in elucidating 16k PRL–mediated functions in antiangiogenic and antitumor mechanisms have been made. Understanding 16k PRL actions in normal physiology as well as abnormal angiogenesis should help in the application of 16k PRL in the treatment of vascular diseases and tumors.

Acknowledgments

Received 3/16/2007; revised 8/31/2007; accepted 9/12/2007.

Grant support: NIH RO1-GM068098 (J. Kunz), RO1-CA111479 (S-H. Lin), and RO1-DK53176 (L-y. Yu-Lee).

The costs of publication of this article were defrayed in part by the payment of page charges. This article must therefore be hereby marked *advertisement* in accordance with 18 U.S.C. Section 1734 solely to indicate this fact.

We thank Dr. Krister Wennerberg for the GST-Rac1G15A vector and Dr. Junji Yamauchi for the GST-Tiam1 RBD vector.

References

1. Bole-Feysot C, Goffin V, Edery M, Binart N, Kelly PA. Prolactin (PRL) and its receptor: actions, signal transduction pathways and phenotypes observed in PRL receptor knockout mice. Endocr Rev 1998;19:225–68.
2. Clapp C, Torner L, Gutierrez-Ospina G, et al. The prolactin gene is expressed in the hypothalamic-neurohypophyseal system and the protein is processed into a 14-kDa fragment with activity like 16-kDa prolactin. Proc Natl Acad Sci 1994;91:10384–8.
3. Piwnica D, Touraine P, Struman I, et al. Cathepsin D processes human prolactin into multiple 16k-like N-terminal fragments: study of their antiangiogenic properties and physiological relevance. Mol Endocrinol 2004;18:2522–42.
4. Corbacho AM, de la Escalera GM, Clapp C. Roles of prolactin and related members of the prolactin/growth hormone/placental lactogen family in angiogenesis. J Endocrinol 2002;173:219–38.
5. Macotela Y, Aguilar MB, Guzman-Morales J, et al. Matrix metalloproteases from chondrocytes generate an antiangiogenic 16 kDa prolactin. J Cell Sci 2006;119:1790–800.
6. Piwnica D, Fernandez I, Binart N, Touraine P, Kelly PA, Goffin V. A new mechanism for prolactin processing into 16k PRL by secreted cathepsin D. Mol Endocrinol 2006;20:3263–78.
7. De Bellis A, Bizzarro A, Pivonello R, Lombardi G, Bellen HJ. Prolactin and autoimmunity. Pituitary 2005;8:25–30.
8. Tworoger SS, Hankinson SE. Prolactin and breast cancer risk. Cancer Lett 2006;243:160–9.
9. Clapp C, Martial JA, Guzman RC, Rentier-Delrue F, Weiner RI. The 16-kilodalton N-terminal fragment of human prolactin is a potent inhibitor of angiogenesis. Endocrinology 1993;133:1292–9.
10. Struman I, Bentzien F, Lee H, et al. Opposing actions of intact and N-terminal fragments of the human prolactin/growth hormone family members on angiogenesis: an efficient mechanism of the regulation of angiogenesis. Proc Natl Acad Sci 1999;96:1246–51.
11. Bentzien F, Struman I, Martini J, Martial JA, Weiner RI. Expression of the antiangiogenic factor 16K hPRL in human HCT116 colon cancer cells inhibits tumor growth in Rag1−/− mice. Cancer Res 2001;61:7356–62.
12. Duenas Z, Torner L, Corbacho AM, et al. Inhibition of rat corneal angiogenesis by 16-kDa prolactin and by endogenous prolactin-like molecules. Invest Ophthalmol Vis Sci 1999;40:2498–505.
13. Kim J, Luo W, Chen D-T, et al. Antitumor activity of the 16-kDa prolactin fragment in prostate cancer. Cancer Res 2003;63:386–93.
14. Tabruyn SP, Sorlet CM, Rentier-Delrue F, et al. The antiangiogenic factor 16K human prolactin induces caspase-dependent apoptosis by a mechanism that requires activation of nuclear factor-κB. Mol Endocrinol 2003;17:1815–23.
15. Lee SH, Nishino M, Mazumdar T, et al. 16-kDa prolactin downregulates iNOS expression through inhibition of the Stat1/IRF-1 pathway. Cancer Res 2005;65:7984–92.
16. Sumpio BE, Riley JT, Dardik A. Cells in focus: endothelial cell. Int J Biochem Cell Biol 2002;34:1508–12.
17. Nobes CD, Hall A. Rho, rac, and cdc42 GTPases regulate the assembly of multimolecular focal complexes associated with actin stress fiber, lamellipodia, and filopodia. Cell 1995;81:53–62.
18. Hall A. Rho GTPases and the actin cytoskeleton. Science 1998;279:509–14.
19. Valster A, Tran NL, Nakada M, Berens ME, Chan AY, Symons M. Cell migration and invasion assays. Methods 2005;37:208–15.
20. Nobes CD, Hall A. Rho GTPases control polarity, protrusion, and adhesion during cell movement. J Cell Biol 1999;144:1235–44.
21. D'Angelo G, Martini J, Iiri T, Fantl W, Martial JA, Weiner RI. 16K human prolactin inhibits vascular endothelial growth factor-induced activation of Ras in capillary endothelial cells. Mol Endocrinol 1999;13:692–704.
22. Galfione M, Luo W, Kim J, et al. Expression and purification of the antiangiogenesis inhibitor 16-kDa prolactin fragment from insect cells. Prot Exp Purif 2003;28:252–9.
23. Garcia GE, Xia Y, Chen S, et al. NF-κB-dependent fractalkine induction in rat aortic endothelial cells stimulated by IL-1β, TNF-α, and LPS. J Leukoc Biol 2000;67:577–84.
24. Benard V, Bokoch GM. Assay of Cdc42, Rac, and Rho GTPase activation by affinity methods. Methods Enzymol 2002;345:349–59.
25. Garcia-Mata R, Wennerberg K, Arthur WT, Noren NK, Ellerbroek SM, Burrudge K. Analysis of activated GAPs and GEFs in cell lysates. Methods Enzymol 2006;406:425–37.
26. Yamauchi J, Miyamoto Y, Tanoue A, Shooter EM, Chan JR. Ras activation of a Rac1 exchange factor, Tiam1, mediates neurotrophin-3-induced Schwann cell migration. Proc Natl Acad Sci 2005;102:14889–94.
27. O'Neill LA. Interleukin I receptors and signal transduction. Biochem Soc Trans 1996;24:207–11.
28. Gao Y, Dickerson JB, Guo F, Zheng J, Zheng Y. Rational design and characterization of a Rac GTPase-specific small molecule inhibitor. Proc Natl Acad Sci 2004;101:7618–23.
29. Liotta LA, Steeg PS, Stetler-Stevenson WG. Cancer metastasis and angiogenesis: an imbalance of positive and negative regulation. Cell 1991;64:327–36.
30. Manser E, Huang HY, Loo TH, et al. Expression of constitutively active α-PAK reveals effects of the kinase on actin and focal complexes. Mol Cell Biol 1997;17:1129–43.
31. Sanders LC, Matsumura F, Bokoch GM, de Lanerolle P. Inhibition of myosin light chain kinase by p21-activated kinase. Science 1999;283:2083–5.
32. Leisner TM, Liu ML, Jaffer ZM, Chernoff J, Parise LV. Essential role of CIB1 in regulating PAK1 activation and cell migration. J Cell Biol 2005;170:465–76.
33. Knaus UG, Morris S, Dong HJ, Chernoff J, Bokoch GM. Regulation of human leukocyte p21-activated kinase through G protein-coupled receptors. Science 1995;269:221–3.
34. Sells MA, Pfaff A, Chernoff J. Temporal and spatial distribution of activated Pak1 in fibroblasts. J Cell Biol 2000;151:1449–58.
35. Lambert JM, Lambert QT, Reuther GW, et al. Tiam1 mediates Ras activation of Rac by a PI(3)K-independent mechanism. Nat Cell Biol 2002;4:621–5.
36. Welch HC, Coadwell WJ, Stephens LR, Hawkins PT. Phosphoinositide 3-kinase-dependent activation of Rac. FEBS Lett 2003;546:93–7.
37. Palacios F, D'Souza-Schory C. Modulation of Rac1 and ARF6 activation during epithelial cell scattering. J Biol Chem 2003;278:17395–400.
38. Mertens AE, Roovers RC, Collard JG. Regulation of Tiam-Rac signaling. FEBS Lett 2003;546:11–6.
39. Etienne-Manneville S. Cdc42—the center of polarity. J Cell Sci 2004;117:1291–300.
40. Kiosses WB, Daniels RH, Otey C, Bokoch GM, Schwartz MA. A role for p21-activated kinase in endothelial cell migration. J Cell Biol 1999;147:831–43.
41. Lee H, Struman I, Clapp C, Martial J, Weiner RI. Inhibition of urokinase activity by the antiangiogenic factor 16K prolactin: activation of plasminogen activator inhibitor 1 expression. Endocrinology 1998;139:3696–703.
42. Gonzalez C, Corbacho AM, Eiserich JP, et al. 16K Prolactin inhibits activation of endothelial nitric oxide synthase, intracellular calcium mobilization and endothelium-dependent vasorelaxation. Endocrinology 2004;145:5714–22.
43. Gho YS, Kleinman HK, Sosne G. Angiogenic activity of human soluble intercellular adhesion molecule-1. Cancer Res 1999;59:5128–32.
44. Chen XL, Zhang Q, Ding X, Tummala PE, Medford RM. Rac1 and superoxide are required for the expression of cell adhesion molecules induced by tumor necrosis factor-α in endothelial cells. J Pharmacol Exp Ther 2003;305:573–80.
45. Han Q, Leng J, Bian D, et al. Rac1-3-p38-2 pathway promotes urokinase plasminogen activator mRNA stability in invasive breast cancer cells. J Biol Chem 2002;277:48379–85.
46. Papapetropoulos A, Garcia-Cardena G, Madri JA, Sessa WC. Nitric oxide production contributes to the angiogenic properties of vascular endothelial growth factor in human endothelial cells. J Clin Invest 1997;100:3131–9.
47. Aranda J, Rivera JC, Jeziorski MC, et al. Prolactins are natural inhibitors of angiogenesis in the retina. Invest Ophthalmol Vis Sci 2005;46:2947–53.
48. Clapp C, Aranda J, Gonzalez C, Jeziorski MC, Martinez de la Escalera G. Vasoinhibins: endogenous regulators of angiogenesis and vascular function. Trends Endocrinol Metab 2006;17:301–7.
49. Hilfiker-Kleiner D, Kaminski K, Podewski E, et al. A cathepsin D-cleaved 16-kDa form of prolactin mediates postpartum cardiomyopathy. Cell 2007;128:589–600.
50. Clapp C, Weiner RI. A specific, high affinity, saturable binding site for the 16-Kilodalton fragment of prolactin on capillary endothelial cells. Endocrinology 1992;130:1380–6.